Physica Medica 64 (2019) 157–165

Contents lists available at ScienceDirect

Physica Medica

journal homepage: www.elsevier.com/locate/ejmp

Original paper

A compressed sensing accelerated radial MS-CAIPIRINHA technique for extended anatomical coverage in myocardial perfusion studies on PET/MR systems

Tobias Wech[a,b,*,1], Karl P. Kunze[c,1], Christoph Rischpler[c,f,g], Daniel Stäb[d], Peter Speier[e], Herbert Köstler[a,b], Stephan G. Nekolla[c,f]

[a] Department of Diagnostic and Interventional Radiology, University Hospital Würzburg, Germany
[b] Comprehensive Heart Failure Centre, University Hospital Würzburg, Germany
[c] School of Medicine, Department of Nuclear Medicine, Technische Universität München, Germany
[d] Siemens Healthcare Pty Ltd, Melbourne, Australia
[e] Magnetic Resonance, Siemens Healthcare GmbH, Erlangen, Germany
[f] DZHK (Deutsches Zentrum für Herz-Kreislauf-Forschung e.V.), Partner Site Munich Heart Alliance, Munich, Germany
[g] Clinic for Nuclear Medicine, University Hospital Essen, University of Duisburg-Essen, Essen, Germany

ARTICLE INFO

Keywords:
Magnetic resonance imaging (MRI)
Compressed sensing (CS)
Projection onto convex sets (POCS)
Positron emission tomography (PET)
Simultaneous multislice (SMS)
MS-CAIPIRINHA
Cardiovascular imaging
Myocardial perfusion

ABSTRACT

Purpose: Simultaneous acquisition of myocardial first-pass perfusion MRI and 18F-FDG PET viability imaging on integrated whole-body PET/MR hybrid systems synergistically delivers both functional and metabolic information on the tissue state. While PET viability scans are inherently three-dimensional, conventional MR myocardial perfusion imaging is typically performed using only three short-axis slices with a temporal resolution of one RR-interval. To improve the integrated diagnostics, an acquisition and image reconstruction method based on "Multi-Slice Controlled Aliasing In Parallel Imaging Results IN Higher Acceleration (MS-CAIPIRINHA)" was developed extending anatomical coverage for MR perfusion imaging to six short-axis slices per RR-interval.
Methods: An ECG-gated radial TurboFLASH MR pulse sequence with dual band excitation was implemented on an integrated whole-body PET/MR system and a model-based reconstruction technique was developed to fully reconstruct the undersampled CAIPIRINHA acquisitions. An 18F-FDG viability PET scan was performed simultaneously to the MR protocol, additionally complemented by a late enhancement MRI acquisition (LGE).
Results and conclusion: The developed imaging technique was tested in five patients with known collateralized coronary total occlusions, resulting in improved characterization of perfusion across areas of decreased tissue viability as indicated by the simultaneously determined 18F-FDG uptake. While conventional MR perfusion with only three slice positions was occasionally missing substantial parts of the viable area, the new approach achieved LV coverage only slightly inferior to LGE imaging and therefore better comparable to PET results. The quality of first-pass enhancement curves was comparable between conventional and radial MS-CAIPIRINHA-based acquisitions.

1. Introduction

The clinically feasible integration of MRI and PET to create a hybrid imaging system has been introduced in 2010 [1,2]. The development was motivated by the vision of combining the excellent spatial resolution and soft tissue contrast of MRI and the distinguished capabilities of PET in molecular imaging at the cellular level [3,4].

Besides a variety of valuable applications in oncology [5], PET/MR imaging bears great potential in particular also for the investigation of cardiovascular diseases [6,7]. The simultaneous, multiparametric assessment of disease in the myocardium in conjunction with high quality anatomical and functional information justifies the expectation that integrated cardiovascular PET/MR can add clinical value with respect to PET/CT or to a sequential MR and PET scan.

* Corresponding author at: Department of Diagnostic and Interventional Radiology, University Hospital Würzburg, Oberdürrbacherstr. 6, 97080 Würzburg, Germany.
E-mail address: wech_t@ukw.de (T. Wech).
[1] Authors have made equal intellectual contributions to the manuscript.

https://doi.org/10.1016/j.ejmp.2019.06.010
Received 29 March 2019; Received in revised form 5 June 2019; Accepted 17 June 2019
Available online 16 July 2019

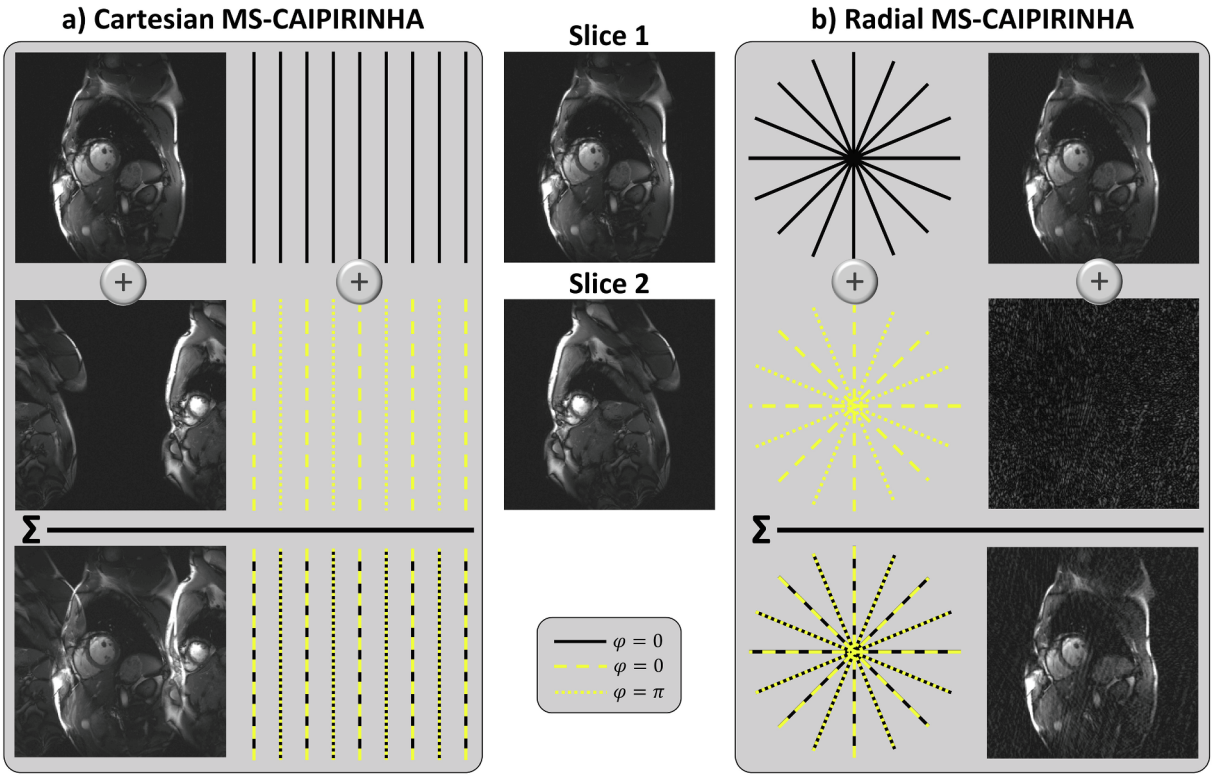

Fig. 1. MS-CAIPIRINHA for Cartesian and radial trajectories. The images in the center represent two parallel fully sampled short-axis slices through the myocardium. The legend indicates the RF-phase, which was toggled between 0 and π in slice 2 for the CAIPIRINHA-acquisitions in (a) and (b).

One of the major issues with this hybrid imaging approach is, however, to achieve an equal anatomical coverage on both the MR and the PET side for a meaningful combined analysis. In myocardial perfusion imaging, for example, MRI delivers high temporal and in-plane spatial resolution; however, conventional saturation-prepared gradient-echo based methods [8–10] typically are only capable of scanning three to four slices per heartbeat with reasonable signal-to-noise ratio (SNR). Conversely, PET myocardial perfusion assessment as well as PET viability imaging are inherently three-dimensional and therefore allow a more complete investigation of the heart. An extension of the anatomical coverage on the MR side is therefore desirable, and different approaches aiming at this goal have recently been proposed: Classical parallel imaging [11,12] is usually already exploited in clinical protocols [10,13,14], however, the achieved acceleration is strictly limited by the inherent noise amplification. “Multi-Slice Controlled Aliasing In Parallel Imaging Results IN Higher Acceleration” (MS-CAIPIRINHA [15]) significantly relaxes this restriction by applying a volumetric multi-slice excitation and sophisticated phase-cycling, which facilitates a parallel imaging-based separation of aliased object information. This technique may be used, for example, to acquire two short-axis slices of the myocardium within the time necessary to scan a single slice at the Nyquist-sampling rate without sacrificing part of the signal-to-noise ratio (SNR) [16].

Furthermore, compressed sensing [17] based techniques may additionally be applied to enable a further increase of acceleration factors in first-pass myocardial MR imaging [18–21]. These methods exploit redundancies within the data by transformation into a domain where they exhibit a sparse representation.

In this manuscript, we propose a Saturation-Recovery (SR) MR first-pass myocardial perfusion measurement technique with extended anatomical coverage for an application on integrated PET/MR systems. The method is based on MS-CAIPIRINHA with radial read-outs and a model-based image reconstruction following the theory of compressed sensing.

MS-CAIPIRINHA-based perfusion measurements were tested in five patients with known collateralized coronary total occlusions against a conventional SR-FLASH perfusion sequence. Both were compared with respect to anatomical coverage and data quality in conjunction with simultaneously acquired 18F-FDG viability PET data as well as Late Gadolinium Enhancement (LGE) images covering the whole left-ventricular (LV) myocardium. In addition, Cartesian MS-CAIPIRINHA was applied instead of the suggested radial approach for two further patients, in order to investigate the expected SNR benefit in the case of radial MS-CAIPIRINHA, previously presented for phantom and head imaging in [22].

2. Theory

2.1. Radial MS-CAIPIRINHA

When using parallel imaging for acceleration of MR data acquisition, the geometry factor g typically represents an important measure for evaluating image quality. If an acceleration factor R with respect to the Nyquist-sampling-rate is used, the signal-to-noise ratio of the reconstructed image ($SNR_{parallel\ imaging}$) is reduced with respect to a fully sampled equivalent image by [11]

$$SNR_{parallel\ imaging} = \frac{SNR_{Nyquist}}{g \bullet \sqrt{R}}$$

The g-factor therefore represents an SNR-loss on top of the inevitable loss due to the reduced number of samples characterized by $\sqrt{R}$. It can be interpreted as a (spatially dependent) measure of how well the parallel imaging algorithm is capable of unfolding pixels, which are aliased due to the accelerated measurement. If the sensitivities of the applied coil array feature low variation for superimposed pixels, the reconstruction problem may be ill-conditioned, ultimately leading to an undesirable increase of g.

CAIPIRINHA represents a technique which elegantly modifies the

RF excitation or k-space sampling pattern to beneficially alter the appearance of aliasing artifacts, thereby maximally exploiting the encoding capabilities of the coil array [15]. In MS-CAIPIRINHA, which is the technique to be used for the proposed MR perfusion measurement, two or more slices are excited simultaneously by a multi-band RF pulse and encoded in an undersampled measurement.

The most straightforward example of a Cartesian dual-band CAIPIRINHA acquisition is illustrated in Fig. 1a. If the two slices were excited simultaneously without any further modification, slice 1 and slice 2 would be superimposed on top of each other within the resulting image (not shown), rendering a separation via parallel imaging challenging if coil sensitivities show only little variation between the possibly adjacent positions in slice direction. In order to address this issue, Cartesian MS-CAIPIRINHA (Fig. 1a) typically applies slice-specific phase-cycling to shift the simultaneously excited slices with respect to each other in image space [15]. In Fig. 1a, the phase of slice 2, i.e. the second band of the RF-pulse, was alternated between 0 and π for consecutive phase encoding steps, shifting the slice by half a field of view (FOV). This results in both a reduction of the average aliasing energy in pixels of the obtained image (bottom of Fig. 1a) as well as a higher variation of coil sensitivities for superimposed information. Therefore, g-factors are typically low, which additionally increases the SNR benefit due to the volumetric/simultaneous excitation [15,23,24].

While information is still aliased in a rather coherent manner for Cartesian MS-CAIPIRINHA, the corresponding application of phase-cycling in radial projection imaging leads to a much more incoherent spread of the information from slice 2 in the resulting image [22] (Fig. 1b). Application of an equivalent pattern (0,π) as in Fig. 1a causes destructive interference in the center of k-space for slice 2. Contrast information is – depending on the grade of undersampling – wiped out and the residual "image" contains only incoherent or noise-like information originating from the periphery of k-space. Multiplying the utilized phase-cycle to the acquired projections, consequentially leads to a constructive depiction of slice two, while the information from slice 1 is superimposed incoherently. As reduced aliasing energy ultimately facilitates a reduction of the *g*-factor with respect to a corresponding Cartesian acquisition [22], radial MS-CAIPIRINHA was used to extend the anatomical coverage in MR perfusion imaging [21] on the PET/MR system in this study. A comparison showing the SNR benefit of radial with respect to Cartesian CAIPIRINHA has been presented recently [25]. For a more detailed description of MS-CAIPIRINHA, the reader is referred to references [15,16,18,22].

2.2. Model-based image reconstruction

Effective parallel imaging reconstruction in conjunction with radial trajectories is facilitated through iterative algorithms [21,22,26]. In order to further enhance image quality in reconstructions of undersampled measurements, an additional sparsity constraint as applied for compressed sensing [17] was used within the algorithm developed for this project. Therein, undersampled data from a radial dual-band acquisition as illustrated in Fig. 1b were subjected to the following optimization to fully reconstruct two images I_1 and I_2:

$$\min_{I_{sl}} \left[\left\| \left(\sum_{sl=1}^{2} \Phi_{sl} E_{sl} I_{sl} \right) - y \right\|_2^2 + \lambda \sum_{sl=1}^{2} \|\Psi I_{sl}\|_1 \right]$$

Here, y corresponds to the measured radial k-space data for all coils. E_{sl} represents the encoding operator, which incorporates an inverse Fourier transform, the re-gridding back to the initial radial projections, and the superposition of the coil sensitivities to obtain multi-coil data. The index *sl* refers to the slice number and runs from 1 to 2 for a dual-band acquisition. Φ_{sl} represents the CAIPIRINHA phase modulation used for the acquisition, and Ψ transforms from image space into the spatial wavelet domain where the images are assumed to be sparse. λ balances the weighting of sparsity and data consistency terms and was chosen empirically for our study. The Wavelet-sparsity term not only suppresses the incoherent artifacts resulting from undersampling as well as from the second slice but also incorporates a de-noising functionality such that overall, the described method is expected to outperform a corresponding Cartesian MS-CAIPIRNHA technique with standard parallel imaging reconstruction with respect to SNR.

We performed the optimization by means of projection onto convex sets (POCS) and implemented the corresponding algorithm in MATLAB (MathWorks, Natick, MA, USA). All reconstructions were executed on an Intel Core i7-3820 CPU @ 3.60 GHz.

3. Methods

3.1. Patient study

For this study, MS-CAIPIRINHA and conventional perfusion imaging datasets were acquired in the context of a cardiac PET/MRI viability protocol on an integrated whole body PET/MR system (Biograph mMR, Siemens Healthcare, Erlangen, Germany). The study was approved by the local ethics committee and all patients gave written informed consent prior to scanning.

Perfusion imaging, LGE and 18F-FDG viability PET were executed during the same scan sessions in seven patients with collateralized coronary total occlusions (CTO, #4: right coronary artery, #2: left anterior descending artery, #1: left circumflex artery). All patients received conventional perfusion imaging, with two of seven receiving additional Cartesian MS-CAIPIRINHA and the other five receiving additional radial MS-CAIPIRINHA perfusion imaging. During patient scans, conventional perfusion acquisition preceded MS-CAIPIRINHA acquisitions, and both were executed after injection of separate boluses of gadolinium-diethylenetriamine pentaacetic acid (Gd-DTPA). This resulted in a split of the full Gd-DTPA dose (0.2 mM/kg) given to each patient into three bolus injections, i.e. two injections of 0.05 mM/kg for the two (conventional and MS-CAIPIRINHA) perfusion scans, and one subsequent injection of the remaining 0.1 mM/kg for LGE imaging. The MS-CAIPIRINHA scan was always performed either in radial or Cartesian mode, so that each patient dataset consisted of one conventional and one MS-CAIPIRINHA acquisition. Execution of three consecutive perfusion scans (conventional as well as both Cartesian and radial MS-CAIPIRINHA) was generally not feasible due to an inacceptable prolongation of the clinical scan protocol. Note that comparability with respect to SNR between perfusion scans from additional consecutive Gd-DTPA injections would have been limited by the elevated level of baseline contrast enhancement from the preceding injections. As the clinical protocol demanded a conventional perfusion scan, Cartesian and radial MS-CAIPIRINHA acquisitions were compared individually to conventional perfusion scans with respect to SNR for example cases only. The main focus of the evaluation described in this manuscript was therefore a comparison between radial MS-CAIPIRINHA and conventional perfusion acquisitions. Both of these approaches were furthermore compared to LGE and PET imaging with respect to LV coverage and the spatial characterization of LGE-positive viability defects. Additionally, enhancement curves from both perfusion acquisitions were qualitatively inspected after signal baseline normalization, in order to compare relative signal behavior in LGE-positive slices.

3.2. Myocardial perfusion MRI acquisition scheme

Fig. 2 illustrates the protocol for imaging first pass myocardial perfusion: Three SR-prepared imaging blocks were acquired per RR-interval for 60–90 consecutive heartbeats under free breathing conditions.

For all MS-CAIPIRINHA acquisitions, dual-band RF pulses were used for excitation with the usual RF spoiling quadratic phase cycle, and an

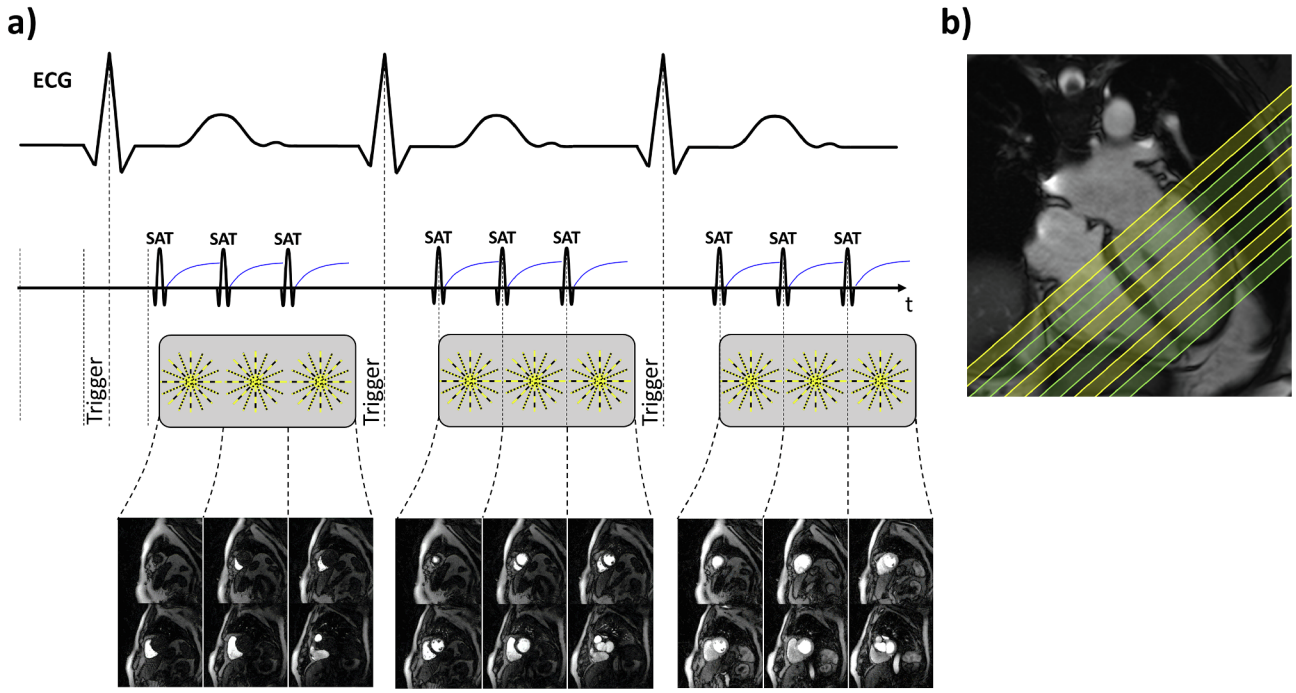

Fig. 2. (a) Imaging protocol for the MR perfusion measurements performed in our study. Three SR-prepared radial dual-slice acquisitions were performed under ECG-gating. The proposed model-based algorithm was then used to reconstruct six short-axis slices per RR-interval. (b) Long-axis view depicting the planning of short-axis views acquired during MR perfusion imaging. Yellow slices show the anatomical coverage of the conventional acquisition technique. Green slices are added by using the presented simultaneous multi slice technique, yielding six short axis slices in total (yellow and green). The additionally performed Cartesian MS-CAIPIRINHA acquisitions followed the same procedure. (For interpretation of the references to colour in this figure legend, the reader is referred to the web version of this article.)

additional RF phase that alternated between 0 an π for the second band (see 2.1 and Fig. 1). For radial sampling, an earlier Cartesian MS-CAIPIRINHA sequence prototype based on TurboFLASH [27] was modified.

Each radial acquisition block consisted of 52 radial projections and a golden angle increment [28] was used for consecutive read outs. This corresponds to an acceleration factor of about 10 with respect to a radial acquisition of two slices obeying the Nyquist sampling rate on a 160×160 grid ($2 \times \pi/2 \times 160 \approx 502$). The respective algorithms, described in Sections 2.2 and 2.1 were then used to reconstruct two short-axis slices for each block as shown at the bottom of Fig. 2. For radial acquisitions, the coil sensitivities for each block and slice *sl* were determined by an oversampled pre-scan under breath hold prior to contrast agent injection. The pre-scan was performed with the same pulse sequence as for the subsequent perfusion measurement, however with just one repetition and 1200 projections for each block / dual-slice. For the two additional Cartesian MS-CAIPIRINHA patient cases, data were acquired with 49 phase encoding steps per block leading to a comparable acquisition time as for the radial approach, and TGRAPPA [29] was used to reconstruct images with a grid size of 192×112 (the second dimension corresponds to the phase encoding direction).

The remaining imaging parameters for both pre- and perfusion-scan are listed hereafter. These were the same for radial and Cartesian acquisitions unless stated otherwise: Gap between adjacent slices = 2 mm, distance between simultaneously acquired slices = 30 mm, slice thickness = 8 mm, total slice coverage = 58 mm, TE = 1.03 ms, TR = 2.33 ms, flip angle = 9-12°, in-plane resolution = 1.88 mm × 1.88 mm (radial) or 2.04 mm × 2.04 mm (Cartesian), image matrix = 160 × 160 (radial) or 192 × 112 (Cartesian).

For comparison, a conventional SR-FLASH perfusion sequence ([30], no MS-CAIPIRINHA acceleration) with Cartesian k-space ordering and three slices per RR-interval was performed with similar sequence parameters as described above (see Fig. 2b for an depiction of the anatomical coverage): Gap between adjacent slices = 8 mm, slice thickness = 8 mm, total slice coverage = 40 mm, TE = 1.03 ms, TR = 2.33 ms, TI = 100 ms, flip angle = 15°, in-plane resolution = 2.04 mm × 2.04 mm, image matrix = 192 × 144, 65 k-space lines using 3-fold GRAPPA with 36 integrated reference lines. No simultaneous multi-slice technique was exploited in this case.

3.3. 18F viability PET

18F-FDG viability imaging after metabolic preparation by intravenous insulin-clamping was performed simultaneously to the MR investigation to optimize myocardial FDG uptake. List-mode PET data were acquired for 45 min starting 60 min after injection of 18F-FDG. Attenuation correction used a 2-point Dixon MRI sequence as previously described [31]. Body parts truncated in the attenuation map due to a limited MRI field-of-view were recovered from PET data using the maximum likelihood reconstruction of attenuation and activity (MLAA) approach [32]. A 3D attenuation-weighted ordered-subsets expectation maximization iterative reconstruction algorithm (AW-OSEM 3D) was used for reconstruction with three iterations and 21 subsets, Gaussian smoothing at 4 mm full width at half maximum, matrix size 344 × 344, zoom 1, and a resulting spatial resolution of 5 mm.

3.4. MRI tissue characterization

After a cumulative dose of 0.2 mM/kg Gd-DTPA and 15 min equilibrium time, LGE imaging was performed with full left ventricular coverage (9–12 slices, slice thickness = 8 mm). Additionally, extracellular volume (ECV) maps were generated at the same three slice positions as the conventional SR-FLASH perfusion acquisition. Therefore, using a Modified Look-Locker Inversion Recovery (MOLLI) sequence, T_1 maps were acquired before (5(3)3-scheme) and 15 min after (4(2)3(1)2-scheme) contrast injection, immediately followed by LGE imaging.

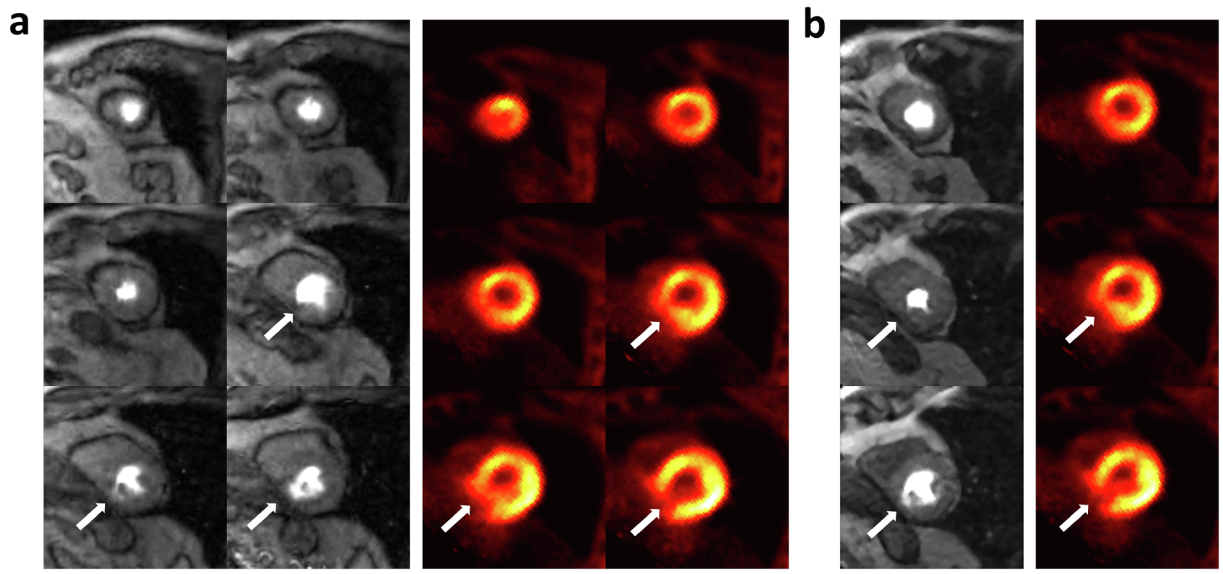

Fig. 3. Radial MS-CAIPIRINHA-based (a) and conventional (b) MR perfusion series in conjunction with corresponding summed 18F-FDG images reconstructed for the same slice positions. Exemplary patient exhibiting an inferior viability defect towards the LV base.

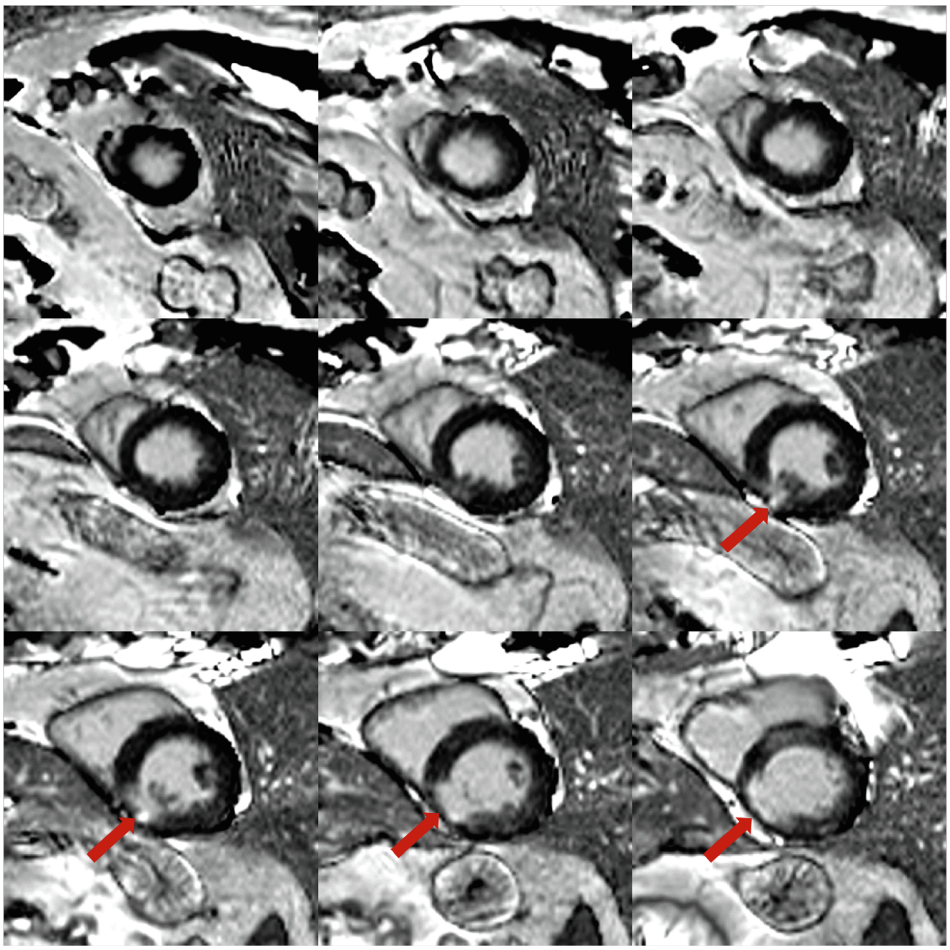

Fig. 4. LGE images acquired across the entire left ventricle of the same patient as in Fig. 3. The medium-sized inferior viability defect is delineated as a hyperintense region corresponding to an increase in extracellular volume.

4. Results

Images from the perfusion series acquired using the proposed radial MS-CAIPIRINHA-based MR technique are shown in Fig. 3a exemplarily for a patient exhibiting a medium-sized defect in the inferior wall.

In Fig. 3b, the same analysis is depicted for the conventional MR perfusion measurement using three short-axis slices. Next to the MR-images, the corresponding 18F-FDG PET images fused to the same

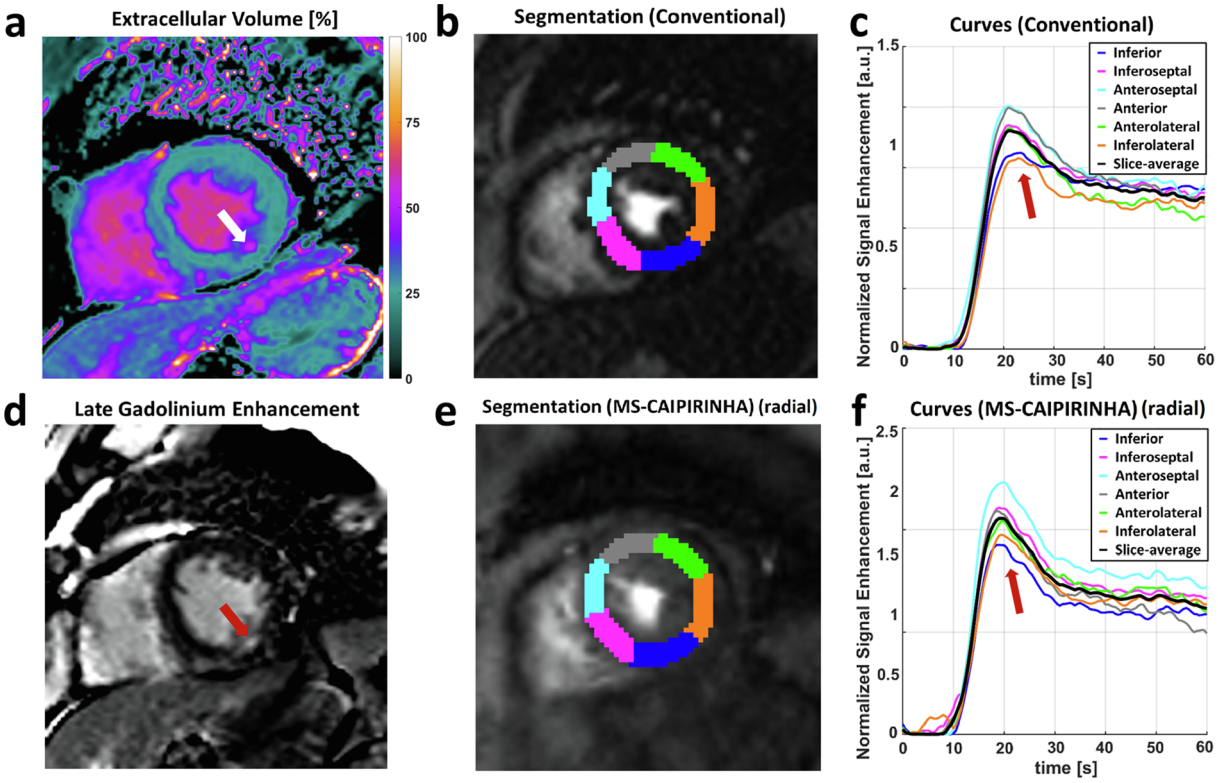

Fig. 5. Extracellular volume (a), LGE (d) and baseline-normalized regional perfusion curves for both conventional (c) and radial MS-CAIPIRINHA-based perfusion imaging (f), with segmentation according to the standard AHA model (b/e). LGE and ECV depict the very subtle inferior/inferolateral viability defect due to a CTO of the RCA, while both perfusion methods show a comparable pattern of decreasing dynamic enhancement in the corresponding territories.

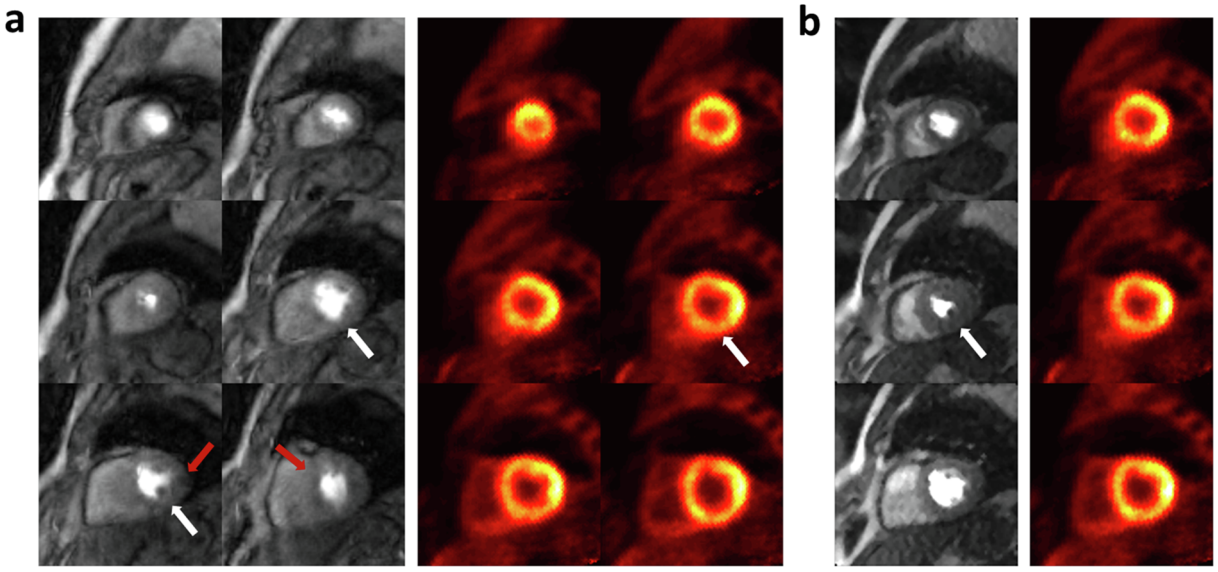

Fig. 6. MR perfusion series and corresponding summed 18F-FDG images for the patient depicted in Fig. 5 exhibiting an RCA CTO. The MR images in (a) were determined by the radial MS-CAIPIRINHA-based method, while those in (b) correspond to the conventional approach. The LGE defect sites are indicated by white arrows, sites of comparably decreased signal quality/homogeneity outside the defect areas using the radial approach are highlighted in red. (For interpretation of the references to colour in this figure legend, the reader is referred to the web version of this article.)

short-axis slice positions are depicted, which are corroborating the viability defect. Fig. 4 complements the evaluation with a presentation of the LGE image series, which was used in conjunction with the metabolic information from the PET data to assess the size of the viability defect. In comparison with the conventional technique (Fig. 3b), the radial MS-CAIPIRINHA-based method (Fig. 3a) enabled an improved characterization of perfusion across areas of decreased tissue vitality as indicated by the simultaneously determined 18F-FDG uptake. While conventional MR perfusion with only three slice positions was missing substantial parts of the viability defect, the new approach achieved an LV coverage (gap between slices = 2 mm), which was only slightly inferior to LGE imaging (Fig. 4, (gap between slices = 0 mm)) and therefore better comparable to 3D PET results. A similar version of Figs. 3 and 4 has been shown in [38].

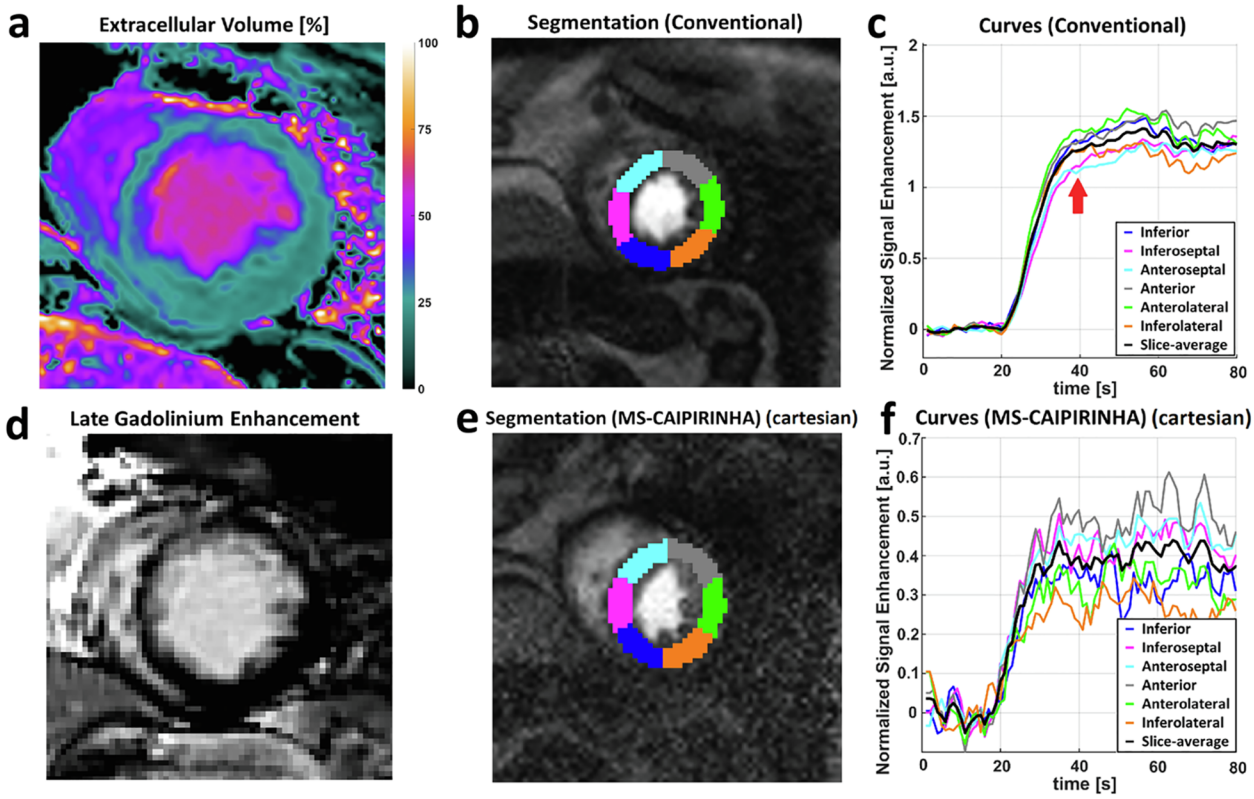

Fig. 7. Baseline-normalized regional perfusion curves for both conventional (c) and Cartesian MS-CAIPIRINHA-based perfusion imaging (f), with segmentation according to the standard AHA model (b/e). Compared to the radial approach (see Fig. 5f), the accelerated acquisition using Cartesian imaging showed a throughout noisier appearance and was not able to characterize the subtle septal perfusion defect highlighted in (c), with the corresponding fibrotic tissue alterations depicted in ECV (a) and LGE images (d). Note also the increased image noise towards the lateral/central image portion in (e).

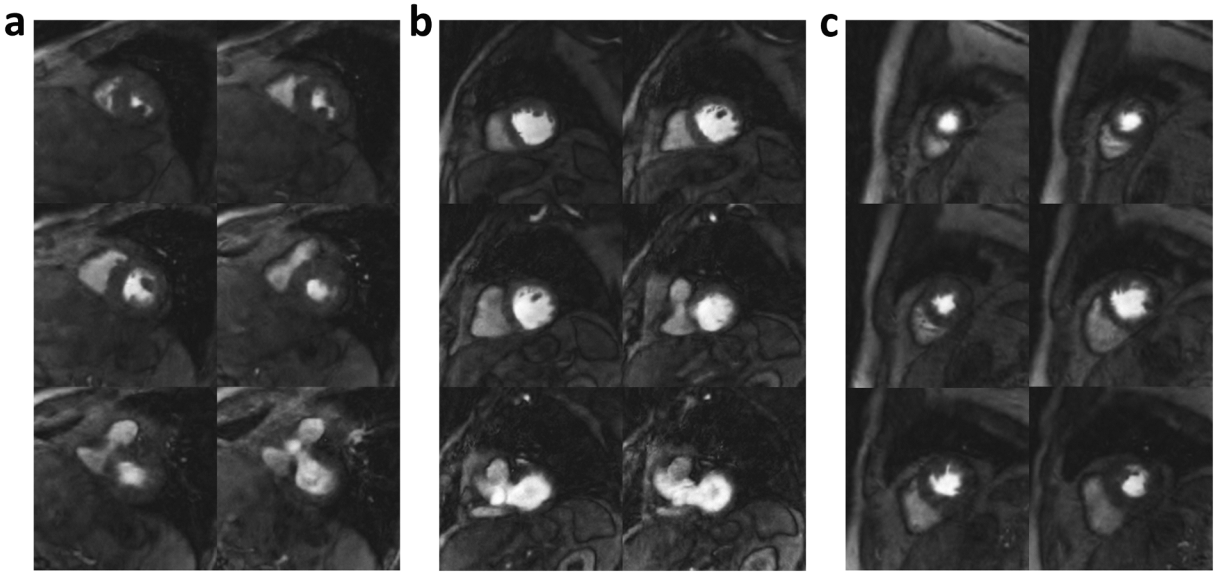

Fig. 8. Overview of the MR-perfusion images for the three remaining patients that received radial MS-CAIPIRINHA imaging.

For the second example patient, a subtle inferolateral defect in the occluded RCA territory is visualized in Fig. 5, both by absolute extracellular volume (a) and LGE (d). In addition, examples for a set of baseline-normalized enhancement curves are shown after segmentation of a mid-ventricular slice according to the standard AHA model for both conventional (b/c) and radial MS-CAIPIRINHA acquisitions (e/f).

These exhibit similarly subtle reductions of dynamic enhancement signal in the inferior/inferolateral regions, concordant with ECV and LGE findings. Note that the baseline-normalized enhancement was lower for the radial MS-CAIPIRINHA curves merely because these were acquired after the conventional perfusion data, i.e. normalization was performed on the basis of significantly higher baseline signals after the first Gd-DTPA injection for the conventional scan. Both sets of regional enhancement curves shown in Fig. 5c/f exhibited comparable data quality and a matching pattern of decreased dynamic signal enhancement in the inferior and inferolateral regions. However, depending on

the relationship between slice positioning and placement of the surface coil array, radial MS-CAIPIRINHA data occasionally resulted in slightly reduced data quality especially at the outer basal/apical slice positions (See e.g. Fig. 6). The comparison of spatial coverage between both perfusion approaches for this patient is also shown in Fig. 6.

The same comparison as shown in Fig. 5 for radial MS-CAIPIRINHA acquisitions was made between conventional and Cartesian MS-CAIPIRINHA perfusion imaging. Fig. 7 shows one of the two cases for which Cartesian MS-CAIPIRINHA data were acquired, visualizing a significant inferiority to the corresponding conventional and radial MS-CAIPIRINHA scan (see Fig. 5f) with respect to SNR. Note that the noisy baseline signal prevented a decent surface coil intensity normalization and enhancement curves did not accurately depict tissue perfusion, which was slightly reduced in the septal wall due to fibrotic alterations shown in corresponding ECV and LGE images (Fig. 5a/d).

Ultimately, Fig. 8 shows an overview of the MR-perfusion studies in the three remaining patients of the study that received radial MS-CAIPIRINHA imaging. The image quality accordingly proved to be constantly high throughout all specimen of the radial approach.

5. Discussion

In the study presented in this manuscript, we have demonstrated the advantages of applying a model-based radial MS-CAIPIRINHA MR technique for myocardial perfusion studies on integrated PET/MR systems. The extension of the anatomical coverage to six short-axis slices per heartbeat has shown potential to beneficially affect the combined analysis of cardiovascular disease. In addition to the more reliable MRI-based estimation of a total ischemic burden, pathologies such as hypoperfusion and matching/mismatching viability defects could be investigated more comprehensively using PET/MRI and the probability of covering also smaller lesions has been significantly improved with respect to conventional techniques. Extension of MRI coverage can also expected to be useful for the assessment of more localized disease effects such as e.g. inflammatory processes in the myocardium using PET/MRI [33] which as a unique multimodal imaging platform for these purposes may only reach its full clinical potential if spatial coverage between PET and MRI is harmonized. For radial MS-CAIPIRINHA, perfusion data quality - as indicated by normalized enhancement curves - was shown to be similar to conventional SR-FLASH perfusion imaging and significantly superior to Cartesian MS-CAIPIRINHA with respect to SNR, confirming the findings for phantom and cerebral studies in [22].

The model that was enforced within the presented reconstruction algorithm for radial MS-CAIPIRINHA data was restricted to the spatial domain (wavelet transform Ψ). As the temporal evolution of the image contrast in perfusion imaging is typically smooth, models exploiting redundancies in the temporal domain [19,21,34] are promising for a further acceleration. In order to evoke incoherent undersampling artifacts through time, however, a temporal alteration of the sampling pattern – which was kept constant in the current study – would be required. This would also allow estimating the needed coil sensitivities from the perfusion measurement itself by reconstructing fully sampled images with reduced temporal resolution.

Alternative techniques for accelerated MR myocardial perfusion were presented in the past. Otazo et al. proposed a low-rank plus sparse decomposition of the spatio-temporal imaging data matrix to enable a separation of background and dynamic information [34]. This proved to be a valuable model within a compressed sensing-based algorithm, inter alia for the reconstruction of undersampled first-pass perfusion measurements. Wang et al. [21] presented a radial MS-CAIPIRINHA method for ungated myocardial perfusion [35], which employed temporal and spatial total variation (TV) constraints within a sparsity enforcing reconstruction algorithm. In contrast to our approach, these techniques also incorporate a model for the temporal domain and therefore have the potential for increased acceleration factors and/or increased SNR. However, enforcing a model within the temporal domain may also increase the risk of overfitting, i.e. temporal smoothing, which can ultimately impair the quality of the perfusion curves [18].

Although, MR and PET data were acquired on an integrated clinical system and at least in parts simultaneously in the presented study, MR and PET images were reconstructed separately. Knoll et al. recently presented an algorithm based on multi-channel regularization, which jointly reconstructs data from both modalities [36]. The advantage of synergistically exploiting anatomical information from all data allowed for an improvement of the resolution and the quantitative accuracy of PET. Furthermore, simultaneously acquired temporally and spatially highly resolved MR data can be used to correct motion and/or partial volume effects on the PET side [37].

6. Conclusion

The proposed radial MS-CAIPIRINHA technique is superior to corresponding Cartesian MS-CAIPIRINHA approaches as well as to conventional single-slice imaging and thus represents a valuable means to extend the anatomical coverage in first-pass myocardial MRI. This is especially favorable in cardiovascular examinations on integrated PET/MR systems, as a joint diagnosis with the simultaneously acquired three-dimensional molecular PET information benefits from an adequate coverage on the MRI-side.

Funding

Deutsche Forschungsgemeinschaft (DFG, Project-ID: KO 2938/4-1).

References

[1] Zaidi H, Ojha N, Morich M, Griesmer J, Hu Z, Maniawski P, et al. Design and performance evaluation of a whole-body Ingenuity TF PET-MRI system. Phys Med Biol 2011;56:3091–106.
[2] Delso G, Furst S, Jakoby B, Ladebeck R, Ganter C, Nekolla SG, et al. Performance measurements of the Siemens mMR integrated whole-body PET/MR scanner. J Nucl Med 2011;52:1914–22.
[3] Quick HH. PET/MR hybrid imaging. Z Med Phys 2017;27:269–70.
[4] Quick HH. Integrated PET/MR. J Magn Reson Imag 2014;39:243–58.
[5] Bailey DL, Pichler BJ, Guckel B, Barthel H, Beer AJ, Botnar R, et al. Combined PET/MRI: from Status Quo to Status Go. Summary Report of the Fifth International Workshop on PET/MR Imaging; February 15–19, 2016; Tubingen, Germany. Mole Imag Biol 2016;18:637–50.
[6] Rischpler C, Nekolla SG, Kunze KP, Schwaiger M. PET/MRI of the heart. Semin Nucl Med 2015;45:234–47.
[7] Robson PM, Dey D, Newby DE, Berman D, Li D, Fayad ZA, et al. MR/PET imaging of the cardiovascular system. JACC Cardiovasc Imag 2017;10:1165–79.
[8] Wilke N, Jerosch-Herold M, Wang Y, Huang Y, Christensen BV, Stillman AE, et al. Myocardial perfusion reserve: assessment with multisection, quantitative, first-pass MR imaging. Radiology 1997;204:373–84.
[9] Atkinson DJ, Burstein D, Edelman RR. First-pass cardiac perfusion: evaluation with ultrafast MR imaging. Radiology 1990;174:757–62.
[10] Coelho-Filho OR, Rickers C, Kwong RY, Jerosch-Herold M. MR myocardial perfusion imaging. Radiology 2013;266:701–15.
[11] Pruessmann KP, Weiger M, Scheidegger MB, Boesiger P. SENSE: sensitivity encoding for fast MRI. Magn Reson Med 1999;42:952–62.
[12] Griswold MA, Jakob PM, Heidemann RM, Nittka M, Jellus V, Wang J, et al. Generalized autocalibrating partially parallel acquisitions (GRAPPA). Magn Reson Med 2002;47:1202–10.
[13] Köstler H, Sandstede JJ, Lipke C, Landschutz W, Beer M, Hahn D. Auto-SENSE perfusion imaging of the whole human heart. J Magn Reson Imag 2003;18:702–8.
[14] Kellman P, Derbyshire JA, Agyeman KO, McVeigh ER, Arai AE. Extended coverage first-pass perfusion imaging using slice-interleaved TSENSE. Magn Reson Med 2004;51:200–4.
[15] Breuer FA, Blaimer M, Heidemann RM, Mueller MF, Griswold MA, Jakob PM. Controlled aliasing in parallel imaging results in higher acceleration (CAIPIRINHA) for multi-slice imaging. Magn Reson Med 2005;53:684–91.
[16] Stäb D, Ritter CO, Breuer FA, Weng AM, Hahn D, Köstler H. CAIPIRINHA accelerated SSFP imaging. Magn Resonance Med 2011;65:157–64.
[17] Lustig M, Donoho D, Pauly JM. Sparse MRI: the application of compressed sensing for rapid MR imaging. Magn Reson Med 2007;58:1182–95.
[18] Stäb D, Wech T, Breuer FA, Weng AM, Ritter CO, Hahn D, et al. High resolution myocardial first-pass perfusion imaging with extended anatomic coverage. J Magn Reson Imag 2014;39:1575–87.
[19] Otazo R, Kim D, Axel L, Sodickson DK. Combination of compressed sensing and parallel imaging for highly accelerated first-pass cardiac perfusion MRI. Magn

Reson Med 2010;64:767–76.
[20] Adluru G, McGann C, Speier P, Kholmovski EG, Shaaban A, Dibella EV. Acquisition and reconstruction of undersampled radial data for myocardial perfusion magnetic resonance imaging. J Magn Reson Imag 2009;29:466–73.
[21] Wang H, Adluru G, Chen L, Kholmovski EG, Bangerter NK, DiBella EV. Radial simultaneous multi-slice CAIPI for ungated myocardial perfusion. Magn Reson Imag 2016;34:1329–36.
[22] Yutzy SR, Seiberlich N, Duerk JL, Griswold MA. Improvements in multislice parallel imaging using radial CAIPIRINHA. Magn Reson Med. 2011;65:1630–7.
[23] Breuer FA, Blaimer M, Mueller MF, Seiberlich N, Heidemann RM, Griswold MA, et al. Controlled aliasing in volumetric parallel imaging (2D CAIPIRINHA). Magn Reson Med 2006;55:549–56.
[24] Breuer FA, Kannengiesser SAR, Blaimer M, Seiberlich N, Jakob PM, Griswold MA. General formulation for quantitative G-factor calculation in GRAPPA reconstructions. Magn Reson Med 2009;62:739–46.
[25] Wech T, Braun M, Stäb D, Speier P, Neubauer H, Kullmann W, et al. Myocardial Perfusion using radial MS-CAIPIRINHA. Ann Meet ISMRM 2016:2607.
[26] Pruessmann KP, Weiger M, Bornert P, Boesiger P. Advances in sensitivity encoding with arbitrary k-space trajectories. Magn Reson Med 2001;46:638–51.
[27] Stäb D, Speier P, Reiter T, Klink T, Neubauer H, Bley T, et al. Restating MS-CAIPIRINHA as an in-plane acceleration problem: an efficient method for integrating high coverage cardiac perfusion MRI into clinical workflow. Ann Meet ISMRM 2015:2686.
[28] Winkelmann S, Schaeffter T, Koehler T, Eggers H, Doessel O. An optimal radial profile order based on the Golden Ratio for time-resolved MRI. IEEE Trans Med Imag 2007;26:68–76.
[29] Breuer FA, Kellman P, Griswold MA, Jakob PM. Dynamic autocalibrated parallel imaging using temporal GRAPPA (TGRAPPA). Magn Resonance Med 2005;53:981–5.
[30] Kunze KP, Rischpler C, Hayes C, Ibrahim T, Laugwitz KL, Haase A, et al. Measurement of extracellular volume and transit time heterogeneity using contrast-enhanced myocardial perfusion MRI in patients after acute myocardial infarction. Magn Reson Med 2017;77:2320–30.
[31] Martinez-Möller A, Souvatzoglou M, Delso G, Bundschuh RA, Chefd'hotel C, Ziegler SI, et al. Tissue classification as a potential approach for attenuation correction in whole-body PET/MRI: evaluation with PET/CT data. J Nucl Med 2009;50:520–6.
[32] Nuyts J, Bal G, Kehren F, Fenchel M, Michel C, Watson C. Completion of a truncated attenuation image from the attenuated PET emission data. IEEE Trans Med Imag 2013;32:237–46.
[33] Rischpler C, Dirschinger RJ, Nekolla SG, Kossmann H, Nicolosi S, Hanus F, et al. Prospective evaluation of 18F-fluorodeoxyglucose uptake in postischemic myocardium by simultaneous positron emission tomography/magnetic resonance imaging as a prognostic marker of functional outcome. Circ Cardiovasc Imag 2016;9:e004316.
[34] Otazo R, Candes E, Sodickson DK. Low-rank plus sparse matrix decomposition for accelerated dynamic MRI with separation of background and dynamic components. Magn Reson Med 2015;73:1125–36.
[35] Chen D, Sharif B, Bi X, Wei J, Thomson LE, Bairey Merz CN, et al. Quantification of myocardial blood flow using non-electrocardiogram-triggered MRI with three-slice coverage. Magn Reson Med 2016;75:2112–20.
[36] Knoll F, Holler M, Koesters T, Otazo R, Bredies K, Sodickson DK. Joint MR-PET reconstruction using a multi-channel image regularizer. IEEE Trans Med Imag 2017;36:1–16.
[37] Petibon Y, Guehl NJ, Reese TG, Ebrahimi B, Normandin MD, Shoup TM, et al. Impact of motion and partial volume effects correction on PET myocardial perfusion imaging using simultaneous PET-MR. Phys Med Biol 2017;62:326–43.
[38] Wech T, Kunze KP, Rischpler C, Stäb D, Speier P, Köstler H. et al. In: Ann Meet ISMRM; 2018, 3681.